INTERNATIONAL ATOMIC ENERGY AGENCY
UNITED NATIONS EDUCATIONAL, SCIENTIFIC AND CULTURAL ORGANIZATION
INTERNATIONAL CENTRE FOR THEORETICAL PHYSICS
I.C.T.P., P.O. BOX 586, 34100 TRIESTE, ITALY, CABLE: CENTRATOM TRIESTE

H4.SMR/650-2

Workshop on Three-Dimensional Modelling
of Seismic Waves Generation
Propagation and their Inversion

30 November - 11 December 1992

Variability of Seismic Ground Motion in Complex Media: The Case of a Sedimentary Basin in the Friuli (Italy) Area

D. Fah (1,3), P. Suhadolc (1), G.F. Panza (1,2),

(1) Istituto di Geodesia e Geofisica, Università degli Studi di Trieste
Via dell'Università 7, 34100 Trieste, Italy

(2) International Centre for Theoretical Physics
Strada Costiera 11, 34100 Trieste, Italy

(3) Institut für Geophysik, ETH Hönggerberg
CH-8093 Zürich, Switzerland

VARIABILITY OF SEISMIC GROUND MOTION IN COMPLEX MEDIA: THE CASE OF A SEDIMENTARY BASIN IN THE FRIULI (ITALY) AREA

D. Fäh [1,3], P. Suhadolc [1] and G.F. Panza [1,2]

(1) Istituto di Geodesia e Geofisica, Università degli Studi di Trieste, Via dell'Università 7, 34100 Trieste.
(2) International Center for Theoretical Physics, Strada Costiera 11, 34100 Trieste.
(3) Institut für Geophysik, ETH Hönggerberg, CH-8093 Zürich.

ABSTRACT

A computational hybrid technique is presented to estimate ground motion in complex two-dimensional, anelastic media. The technique combines modal summation and finite difference methods, and it can take into account the source, path and local soil effects to calculate the local wavefield due to a seismic event.

The hybrid technique is applied to study wave propagation in a sedimentary basin in the Friuli region during the September 11, 1976, Friuli aftershock ($16^h35^m04^s$). Special emphasis is given to the understanding of the different features of ground motion in sedimentary basins. The most important effects that can be observed are the excitation of local surface waves at lateral heterogeneities, and local resonances. Within the sedimentary basin studied, the coda of the transverse component is mainly composed of the local, fundamental-mode Love wave, whereas the P-SV wavefield shows dominant contributions of the higher modes of Rayleigh waves. These differences in wave composition lead, in general, to different dispersion characteristics and attenuation phenomena for SH and P-SV waves. A parametric study demonstrates the sensitivity of the computed ground motion to small changes in the subsurface topography of the sedimentary basin, and the velocity and

quality factor of the sediments. The results obtained for one- and two-dimensional structural models show that only two-dimensional structural models are suitable for the prediction of complete seismic ground motions in sedimentary basins, because they can account for the generation of local surface waves.

To establish the validity of the numerical results, they are compared with observed ground motion. The relative amplitudes, durations, and frequency content of the different components of the synthetic signals agree well with the observations.

Keywords: wave propagation modelling, seismic strong ground motion, sedimentary basins.

INTRODUCTION

Numerical simulations play an important role in the estimation of ground motion in regions of complex geology. In engineering seismology, they can provide synthetic signals for areas where recordings are absent and are therefore very useful for design of earthquake-resistant structures. In seismic reflection or refraction studies, numerical simulations provide a means for interpretation of seismic sections. For applications in seismic studies, it is generally sufficient to treat wave propagation in laterally heterogeneous structures with asymptotic forms for high frequencies. These methods, termed as "ray methods", can only be applied to smoothly varying media in which characteristic dimensions of the inhomogeneities are considerably larger than the prevailing wavelength. They fail, however, to predict ground motion at sites close to lateral heterogeneities such as edges of sedimentary basins and at sites above irregular bedrock-sediment interfaces, where excitation of local surface waves and resonance effects can become important. Therefore, it is necessary to justify the validity of the selected method, relative to whether the structure of the site under consideration falls within the domain of the method.

Far away from lateral heterogeneities, a local structure can sometimes be approximated by a horizontally-layered structural model. In this case of a one-dimensional structure, the mode summation method is a powerful tool for computing broadband synthetic seismograms. The mode summation method is still suitable when lateral variations can be schematized with vertical discontinuities (Vaccari et al., 1989), but it is presently not applicable to local irregular structures, which cannot be reduced to plane-layered models. Since high-frequency seismograms are very sensitive to lateral heterogeneities, the influence of these local and irregular heterogeneities should be included in the numerical modelling. A powerful method for simulating wave propagation in two-dimensional media is the computational hybrid technique presented in this study. The hybrid method combines modal summation and the finite difference technique (Fäh et al., 1990; Fäh, 1992). It can include both a realistic source model and a complex structural model such as a sedimentary basin, without the restriction to asymptotic forms for high frequencies.

In the following, this method is applied to simulate a seismic event in the Friuli seismic region, and the results are used to study the wave propagation effects in the Friuli sedimentary basin. One major problem of such numerical simulations is the enormous number of parameters which have to be specified as input. The choice of these parameters is based on all available seismological, geological and geotechnical information for the area under consideration. Our numerical simulation predicts the seismic response at a specific site, only if the mechanical parameters (density, velocity, damping, etc.) and geometrical parameters (such as thickness) are reasonably well-known. Due to the restriction to two-dimensional models, and the limited knowledge about the structure and the seismic source, it is in general not possible to define one single structural model. Moreover, waveforms are also sensitive to small changes of the structural model close to the receiver, especially within sedimentary basins, where the influence of the lateral heterogeneities on wave propagation is very strong.

In this study, we will focus on the variability of ground motion. Special attention is paid to the types of waves generated inside sedimentary basins, to the differences between results obtained for one- and two-dimensional structural models, and the limits of numerical modelling imposed by the use of two-dimensional structural models. The results of the numerical simulations are compared with observed ground motion to establish the validity of the numerical results.

THE HYBRID METHOD

The hybrid method uses each of the two techniques in that part of the structural model where it works most efficiently: the finite difference method is used in the laterally heterogeneous part of the structural model which contains the sedimentary basin (see Figure 1), and modal summation is applied to simulate wave propagation from the source position to the sedimentary basin or the local irregular feature of interest. This hybrid approach allows us to calculate the local wavefield from a seismic event, both for small (a few kilometers) and large (a few hundreds of kilometers) epicentral distances. The use of the mode summation method allows us to include an extended source, which can be modelled by a sum of point sources appropriately distributed in time and space. This allows the simulation of a realistic rupture process on the fault. The path from the source position to the sedimentary basin can be approximated by a structure composed of flat, homogeneous layers. Modal summation then allows the treatment of many layers which can take into consideration low-velocity zones and fine details of the crustal section under consideration. The finite difference method, applied to treat wave propagation in the sedimentary basin, permits the modelling of wave propagation in complicated and rapidly varying velocity structures. The coupling of the two methods is carried out by introducing the resulting time series obtained with the mode summation method into the finite difference computations. In the SH computations the displacements are used as input in the finite difference calculations, whereas in the P-SV case the input consists of the velocity time series.

In the mode summation method, the treatment of P-SV waves is based on Schwab's (1970) optimization of Knopoff's (1964) method (Panza, 1985), and the handling of SH waves is based on Haskell's (1953) formulation (Florsch et al., 1991); these computations include the "mode-follower" procedure and structure minimization described by Panza and Suhadolc (1987). The introduction of anelasticity into the computations is based on variational methods (Takeuchi and Saito, 1972; Schwab and Knopoff, 1972), and includes Futterman's (1962) results concerning the dispersion of body waves in a linearly anelastic medium. By comparison with the results obtained from the exact treatment of anelasticity (Schwab, 1988; Schwab and Knopoff, 1971; 1972; 1973), the attenuation effects obtained from the variational technique turn out to be in error by about 20 percent, a value certainly acceptable for our purposes.

The seismic source is introduced by using the Ben-Menahem and Harkrider (1964) formalism. These far field expressions are valid, if the distance from the source, Δ, is larger than the dominant wavelength, λ, of the computed signal; if $\Delta>\lambda$, the first term of the asymptotic expansion of the cylindrical Hankel functions, appearing in the far field expressions, is exact with at least three significant figures (Panza et al., 1973). The seismograms computed with modal summation contain all the body waves and surface waves, whose phase velocities are smaller than the S-wave velocity of the half-space that terminates the structural model at depth. These computations therefore supply a realistic incoming wave-field, to be used as input in the finite-difference computations.

Explicit finite difference schemes are used to simulate the propagation of seismic waves in the sedimentary basin. These schemes are based on the formulation of Korn and Stöckl (1982) for SH waves, and on the velocity-stress, finite difference method for P-SV waves (Virieux, 1986; Levander, 1988). The algorithms can handle structural models containing a solid-liquid interface, and are numerically stable for materials with normal, as well as high values of Poisson's ratio.

Intrinsic attenuation in soft sediments is an important process and should always be taken into account to prevent serious errors in the simulation of wave propagation in sedimentary basins. In the finite difference computations, anelasticity is included using the rheological model of the generalized Maxwell body. The numerical algorithm has been developed by Emmerich and Korn (1987) for the case of SH-wave propagation, and it has been extended to the P-SV case by Fäh (1992) and Emmerich (1992). In this method, the viscoelastic modulus is approximated with a low-order rational function of frequency. This approximation can account for a constant quality factor over a certain frequency band. Replacement of all elastic moduli by viscoelastic ones, and considering the stress-strain relation in the time-domain, yields a formulation which can be handled with a finite difference algorithm.

The limits of the hybrid technique are imposed by the need for relatively large amounts of CPU time and computer memory in the finite difference computations. The finite difference method has the disadvantage that limitations of computer memory require the introduction of artificial boundaries, which form the border of the finite

difference grid in space. These boundaries are a severe problem in finite difference methods, since they can generate spurious reflections of the waves impinging upon them from the interior of the grid. Therefore, before going into two-dimensional computations, we first compare the results of modal summation and the finite difference technique for the simple case of a one-dimensional structural model. This comparison is necessary each time the hybrid technique is applied in a new region. The comparison allows us to establish control over the accuracy of the finite difference part of computations, relative to: (1) the efficiency of the absorbing, artificial boundaries, (2) the correct discretization of the structural model in space, (3) the presence of all phases in the seismograms, and (4) the treatment of anelasticity. The comparison is performed for the same layered structural model which describes the path from source position to the region where the finite difference method is applied. An important disadvantage of the hybrid technique is the fact that geometrical spreading cannot be treated in the finite difference computations in an exact manner; despite this problem, from the one-dimensional experiment we can estimate the lower bound of error in the hybrid technique to be 2 to 5 percent in amplitudes with respect to modal summation (Fäh, 1992). This error is valid for the source-receiver distances considered in the numerical examples (Figure 1), and it can only be obtained if the discretization in space is optimized, and if the finite difference grid is deep enough to guarantee the completeness of the signals. This lower error bound for the hybrid method can be expected for any laterally heterogeneous structure, and the low value of this bound allows the application of the hybrid technique to the study of wave propagation in sedimentary basins with relatively high accuracy.

EXAMPLES OF NUMERICAL MODELLING

The September 11, 1976 Friuli aftershock ($16^h35^m04^s$) has been recorded by a few accelerographic stations (CNEN-ENEL, 1977). Records from one of the nearest stations -- the three-component records at station Buia -- will be considered and compared with theoretical computations. The low-pass filtered accelerograms recorded at station Buia are shown in Figure 2a. They are not corrected for the instrumental response.

The area where the station of Buia is placed is characterized by terrigenous sediments (Flysch), widely outcropping at Monte Buia (Figure 3). They are covered locally by a thin quaternary layer, forming a sedimentary basin, and overlap a carbonatic mesozoic sequence. The surface sediments are incoherent, of glacial, alluvial, and lacustrine origin (Barnaba, 1978). They form the so-called Amphitheater of the Tagliamento river. The thicknesses of the quaternary sediments are well-known (Giorgetti and Stefanini, 1989) and locally can reach 100 m. At station Buia they reach a thickness of about 57 m.

NUMERICAL MODELLING FOR A ONE-DIMENSIONAL STRUCTURAL MODEL

Assuming a one-dimensional, layered, anelastic structural model for the region, Panza and Suhadolc (1987) have shown that the observed signals at station Buia for the September 11, 1976 earthquake cannot be explained by only a single point source. They used the mode summation technique to reproduce the observed vertical component, by trial-and-error varying of a set of source parameters. A good fit was obtained with three point sources having different weights and time shifts, but the same focal depth, mechanism, and duration. The same conclusion was drawn by modelling all three recorded components (Figure 2b), and combining SH and P-SV waves (Florsch et al., 1991). In the last study, the source is approximated by a sum of six point sources, still modelling three different rupturing episodes. The parameters varied in the process were the number of point sources, their origin time, and the weights of the individual sources. The source-receiver distance, the source depth, the strike, dip and rake were varied, but kept constant for all subevents. All these parameters were adjusted until a satisfactory waveform fit was obtained, both in the time and in the frequency domain. This fitting was limited to frequencies below 6.5 Hz.

The one-dimensional layered, anelastic structural model used, is representative of the Friuli area (model FRIUL7W in Table 1). It is essentially based on a damped, least-square inversion of arrival time data from local earthquakes (Mao and Suhadolc, 1987; 1992). In the model FRIUL7W, the thickness of the surficial sediments corresponds to their thickness at station Buia (Giorgetti and Stefanini, 1989).

In all cases of waveform fitting, the orientation of the sources agrees well with previously published results by Slejko and Renner (1984), who interpreted the event as one of thrust on a very shallow, NW dipping plane. Several point sources with different weights and time shifts are required to fit the observed signals (Figure 2b). The vertical component can be well reproduced, whereas the synthetic NS-component has excessively large amplitudes in the coda. The duration of the observed EW-component cannot be explained by this set of point sources. The difficulty in reproducing the observed horizontal components of motion with a one-dimensional structural model arises from the fact that local lateral heterogeneities are the main influence on these components. On the other hand, the vertical component of motion is much less affected by local site conditions and can be modelled quite well with one-dimensional structural models.

NUMERICAL MODELLING FOR TWO-DIMENSIONAL STRUCTURAL MODELS

The effect of the sedimentary basin is studied with the hybrid approach and represents an application of this technique for frequencies from 0.5 Hz to 6.5 Hz. The dominant energy of the observed signals is contained in this frequency band. The lower frequency limit (0.5 Hz) is chosen in order to neglect the higher-order cylindrical Hankel functions in the source expression (Panza et al., 1973). The higher frequency limit (6.5 Hz) is introduced because of the chosen grid spacing selected in the finite difference computations. The number of grid points in the finite difference computations is 750x300. The mesh size is 10 m by 10 m in the upper part of the model and 10 m by 30 m in the lower part, resulting in a model size of 7.5 by 7.0 km.

The depths to the bedrock in the sedimentary basin are taken from the work published by Giorgetti and Stefanini (1989). For the definition of the seismic P-wave velocities of the quaternary sediments, results from refraction measurements in the region of Madonna di Buia (Giorgetti, 1976) and different parts of the Amphitheater (Martinis et al., 1976) were taken. The variability of shear-wave velocities is known from cross-hole measurements in the Tarcento region (Brambati et al., 1980). The mechanical properties of the quaternary sediments vary between

$\rho=1.8$ g/cm^3, $\alpha=1.3$ km/s and $\beta=0.35$ km/s near the surface, and $\rho=2.0$ g/cm^3, $\alpha=1.8$ km/s and $\beta=0.8$ km/s at larger depths.

We are restricted to two-dimensional models, but the real structure -- mainly the depth of the sediments and their mechanical properties -- varies in the horizontal plane. In 2D modelling, this can be accounted for partly by studying the wave propagation along different cross-sections. Their positions are shown in Figure 3, and the related two-dimensional structural models are presented in Figure 4. The main features of cross-section A are two sedimentary basins intersected by the outcropping of Flysch at Monte Buia. Cross-section B represents an average model for the region, whereas cross-section C represents the part of the Amphitheater with deep sediments. Cross-section D is chosen to be very simple, having only a sharp vertical discontinuity between two layered quarter-spaces: the first corresponding to layered structure FRIUL7W without the sedimentary layer, the second to FRIUL7W with the sedimentary layer. The thickness of the sedimentary layer is equal to the thickness (57m) of the quaternary sediments at station Buia.

The layered one-dimensional model, describing the propagation of waves from the source position to the sedimentary basin, is chosen to be the model FRIUL7W (Table 1) without the sedimentary cover of 57 m thickness. The source is always placed in the plane of the cross-section, and the source depth, mechanism, and duration are those of the first source considered by Florsch et al. (1991) (source-depth 7.1 km, angle between the strike of the fault and the epicenter-station line 19°, dip 28°, rake 115°, and source duration 0.6 s).

The first example of computations with the hybrid technique is the simulation of wave propagation in the two-dimensional structure corresponding to cross-section A (Figure 4). The accelerograms for an array of receivers at the surface of this structure is shown in Figure 5. Heterogeneities with size comparable to the wavelength of the incident wavefield generate significant spatial variations of the ground motion. They act on the wavefield as would fictitious sources placed at the location of the heterogeneities themselves. The closer they are to the observation point the more important are the effects. Even for closely neighboring sites, it is possible to observe big differences in shape, duration, and frequency content of the signals.

At the first station (9.8 km from the source) the sediments are shallow. The influence of this thin sedimentary cover on wave propagation is not important since the characteristic dimensions of the inhomogeneity are considerably smaller than the prevailing wavelength. The high-frequency part of the P-SV wave energy is concentrated in the radial components. When the sediments become thicker the energy is redistributed by diffractions, and by multiple reflections in the sedimentary layer. The multiply reflected body waves can dominate the shape of the signals and, after a short propagation path, form local surface waves (phases L_1, R_1 and R_2). They are the dominant phase for P-SV waves (phase R_2) and have much smaller amplitudes for SH waves (phase L_1). In the P-SV case, the dipping layer at the edge of a sedimentary basin gives rise to different types of local surface waves: the fundamental mode (phase R_1) which is prominent on the vertical component, and the first higher modes (phase R_2). For the SH case, on the other hand, the coda of the signals is composed almost completely of the fundamental mode Love-wave. The extension of the zone in the sedimentary basin, within which these local surface waves are of considerable amplitude, depends on the waves' frequency content and the quality factor of the sediments. The lower are the frequencies and the higher is the quality factor, the larger is the extension of the zone where local surface waves are of considerable amplitude. The frequency content of local surface waves, at a given distance from the edge of the basin, depends on the inclination of the bedrock-sediment interface and the thickness of the sediments. Since the depth of the sedimentary cover does not remain constant, the group velocity of the local surface waves can vary and mode conversions can occur within sedimentary basins.

The amplitudes of the reflected waves at the right edge of the first basin are small. They interfere with local surface waves excited by the direct body-waves at the right edge of the sedimentary basin. The amplitudes of these waves are also very small. Resonance effects of the surface layer dominate the shape of the signals at all stations inside the sedimentary basin. The predominant periods of the signal at each station are related to the thickness of the sedimentary layer. A good example of a strong local resonance can be seen on the transverse component (at 11.8 km from the source) with an arrival time of about 3 s and with dominant frequencies around 5 Hz. This special type of resonance at the edges of the sedimentary basins can often be observed in theoretical computations (Fäh et al., 1990). They can probably be related to the effects reported for earthquakes, where severe damage has been observed at the edges of sedimentary basins, e.g. the concentration of damage observed during the Skopje, Yugoslavia earthquake of 1963 (Poceski, 1969).

On the outcrop, the signals loose most of the high-frequency content and the amplitudes are smaller than elsewhere. Local surface waves are also excited in the second sedimentary basin (located after the outcrop with respect to the source), but now also with great amplitudes on the transverse component. These local surface waves are mainly formed by trapped S-waves interfering constructively for frequencies around 2 Hz. These frequencies are close to the first mechanical resonance frequency of an infinite layer whose thickness and mechanical properties are equal to those of the sedimentary layer in its thicker part. A characteristic of these local surface waves is their strong dispersion, which can be explained by the group velocity curve shown in Figure 6 for the corresponding layered model FRIUL7W. On the transverse component, there is an excitation of local surface waves corresponding to the fundamental Love mode with frequencies near those of the minimum in the group velocity curve. This wavetrain never separates from the direct wavetrain. The lowest velocity corresponds to the minimum group velocity (0.40 km/s) of the fundamental mode.

As was observed in the SH case, in the second sedimentary basin, there is also excitation of local Rayleigh waves with frequencies lower than that of the group velocity minimum. The interpretation of the P-SV seismograms is more difficult than it is for SH waves. From the group velocity curves, shown in Figure 6, it should be expected that not only the fundamental mode is locally excited, but also some of the higher modes. Close to the frequency of 2 Hz, there is an apparent continuity of the group velocity between adjacent modes. This mode-to-mode continuation leads to an almost continuous group velocity which begins with the first higher mode and contains segments of all successive higher modes. The superposition of these higher modes leads to the large amplitudes that are observed in the coda of the signals.

COMPARISON OF COMPUTED GROUND MOTION WITH OBSERVATIONS

The computations have been made also for the cross-sections B and C, for the model with two quarter-spaces (cross-section D), and the one-

dimensional model FRIUL7W (cross-section MOD). For the specific site of station Buia, we will analyse the differences due to the use of different structural models. At station Buia, which is 15 km distant from the source, the thickness of the sedimentary cover is the same for all models. A comparison is shown in Figure 7 between the transverse, radial and vertical components of ground motion computed for the five different cross-sections of the basin, and the observed accelerations at station Buia.

The local Love waves -- in the text, also referred to as the 2 Hz surface waves -- never separate from the direct wavetrain (see transverse component in Figures 5). From the group velocity curves (Figure 6) and the strong dispersion of the coda, which has a dominant frequency around 2 Hz, we have concluded that this wavetrain is mainly fundamental-mode energy. Owing to its strong attenuation, this wavetrain does not propagate over large distances. The fundamental-mode Love wave can be excited at the edge of the sedimentary basin or at lateral heterogeneities within the sedimentary basin. For model D, formed with just two quarter-spaces, lateral heterogeneites inside the basin are absent; thus at larger distances from the edge of the basin, the local Love waves are strongly attenuated (ND in Figure 7). In the case where the interface between the bedrock and the sediments approaches the free surface (cross-section B and C), or in the case of an outcropping of the bedrock (cross-section A), the local 2 Hz surface waves are also generated by these heterogeneities. For cross-sections B and C, several phases with local surface waves, excited at different heterogeneities, can interfere.

The first part of the observed transverse component resembles the first part of the signals obtained for model D, and for the one-dimensional model MOD. In the coda of the observed signal, however, there is evidence for local surface waves generated by the sedimentary basin. The synthetic seismograms, obtained for the one-dimensional model (label MOD), cannot reproduce the waveform and duration of the observed signal. This can be explained by the fact that local surface waves cannot be excited in a laterally-homogeneous, layered structural model. The local surface waves, obtained for cross-sections A, B and C, have amplitudes that are too large in comparison with the observed signals. In the choice of the geometry of the bedrock-sediment interface, we have restricted ourself to the geometry given by Giorgetti and Stefanini (1989). However, to reproduce the observed transverse component, the heterogeneities inside the sedimentary basins, responsible for the excitation of these local surface waves, would have to be different from those used in the numerical modelling. The heterogeneities are either too close to station Buia or the bedrock-sediment interfaces are too close to the free surface. Good agreement with the observed transverse acceleration can be obtained for the simplest model, D. On the other hand, the rather large amplitudes of the surface waves in the observed signals can be explained if we assume an excitation of local surface waves within the sedimentary basin.

For the radial component of ground motion, the situation with the excitation of local surface waves is not as clear as it is for Love waves. In the P-SV case there are also three sources of local surface waves: the edge of the sedimentary basin, the places where the bedrock-sediment interface approaches the free surface, and the outcropping of the bedrock. From the signals obtained for cross-sections A, B and C, it can be concluded that the stronger the lateral heterogeneity within the basin is, the greater are the amplitudes of the local Rayleigh waves. On the other hand, these lateral heterogeneities can reflect most of the local Rayleigh waves coming from the edge of the sedimentary basin closest to the seismic source.

The comparison of the synthetic signals with the observed radial component shows good agreement between that observation and the signal obtained for cross-section C. Due to the small amplitudes of the coda in the observed radial component, it can be concluded that the local surface waves have travelled through the deeper parts of the sedimentary basin and that the lateral heterogeneity within the basin has reflected the local surface waves from the first edge of the basin. To reproduce the observed signal, the lateral heterogeneity within the basin cannot be strong; a strong heterogeneity, in fact, would excite large-amplitude local surface waves inside the basin, and these are not observed experimentally. No agreement can be found between the observed radial acceleration and the synthetic signal obtained with modal summation for the one-dimensional, layered structural model.

Comparison between the observed vertical component of ground motion and the synthetic signals shows that for the lower-frequency part (below 4 Hz) of the signals, there is less difference between the vertical components of motion than it was observed for the horizontal ones. This similarity of the vertical components of motion is a fact that was also observed at different sites in Mexico City during the 1985 Michoacan

earthquake (Campillo et al., 1988), and therefore, on the basis of our calculations, it can be considered a quite general property. The high-frequency ringing not observed experimentally but present in the synthetic signals for models A, B and C, is the remainder of the resonance effects in the shallow part of the sedimentary cover. This difference once again indicates, that in the numerical modelling, the shallow parts of the sedimentary cover are too close to the observation point, or the bedrock-sediment interfaces are too close to the free surface.

The relative amplitudes of the different components of the synthetic signals agree well with the observed signals. Assuming a point source, the long duration of the signals can be explained by local surface waves, even though an approximation of the magnitude $M_L=5.7$ earthquake with a point source might not seem realistic. There is evidence for the generation of surface wave energy at the first edge of the sedimentary basin and at lateral heterogeneities within the basin. Therefore, it can be concluded that the complexity of the source proposed by Florsch et al. (1991) is only partly real, and is partly an artifact of their assumption of a laterally homogeneous structure.

SENSITIVITY OF THE SIGNALS TO CHANGES OF THE QUALITY FACTOR AND OF THE SHEAR WAVE VELOCITY OF THE SEDIMENTS

In the previous section, we have seen that waveforms of synthetic signals are sensitive to small changes in the subsurface topography. We now want to focus on the influence of the local surface-soil properties, i.e. on the influence of shear-wave velocity and quality factor in the sediments. For our computations, average structural model B has been chosen. The results obtained for different shear-wave velocities are shown in Figure 8, where the three components of motion are compared with the records at station Buia.

The horizontal components of motion are very sensitive to small changes in shear-wave velocity, whereas the vertical component in its low-frequency part (below 4 Hz) shows smaller differences. The lower the shear-wave velocity of the sediments, the larger the amplitudes of the local surface waves, and the stronger their dispersion. The effects are more evident in the case of SH waves due to the dominant contribution of the fundamental-mode Love wave. The increased spatial attenuation due to the low shear-wave velocities reduces the high-frequency content of the synthetics. The maximum amplitude of the first body-wave pulse changes only slighly.

The influence of the quality factor on ground motion is shown in Figure 9. The synthetic signals have been computed for three different quality factors Q_β of the sediments, by keeping the shear-wave velocity fixed at 0.6 km/s. The amplitudes of the local surface waves are more and more attenuated as the quality factor decreases. Since the heterogeneity which is mainly responsible for the local surface waves is about 1 km from the receiver, a quality factor as low as 5 damps out the local surface waves almost completely. What remains in this case, is the one-dimensional response of the local structure just below the receiver, and the duration of the signals become similar to that of the synthetics obtained with the one-dimensional structural model (label MOD in Figure 7).

CONCLUSIONS

The examples considered in our study have shown the well-known amplification of the incident waves, which occurs when a seismic wave travels through an interface from a medium with relatively high rigidity, into a medium of lower rigidity. Sloping interfaces, such as the transitions from bedrock to sediments, can generate local surface waves in the sedimentary layers. These local waves can dominate the seismic signal, especially close to the transition zone. Their energy propagates mainly in the sedimentary layer. For both SH and P-SV waves, strong resonances can occur in parts of the basins with smooth variations of the geometry of the interface between bedrock and sediments. In general, the behavior of SH waves and P-SV waves in sedimentary basins is different. This is due to the different frequency content of the two classes of waves, and different physical processes, e.g. the S- to P-wave conversion for P-SV waves at strong impedance contrasts. Within the sedimentary basin studied, the coda of the transverse component is mainly composed of the local, fundamental-mode Love wave, whereas the P-SV wavefield shows dominant contributions of the higher-modes Rayleigh waves. The superposition of these higher modes leads to the large amplitudes that are observed in the coda of the signals. These differences in wave composition

lead to different dispersion characteristics and attenuation phenomena for SH and P-SV waves.

An important test of any numerical result is the comparison between the synthetic signals and the observed ground motion, which allows us to establish validity of the numerical results. The synthetic signals can explain the major characteristics of the observations. For selected structural models, the relative amplitudes, durations, and frequency content of the different components of the synthetics agree well with the recorded data. In general, there is considerable variability of synthetic ground motion for different, realistic two-dimensional models of a sedimentary basin. The theoretical study shows that waveforms and frequency content of computed seismograms are sensitive to small changes in the subsurface topography of the sedimentary basin, and the velocity and quality factor of the sediments. This has also been noted experimentally for records from different sites in existing strong-motion arrays. What remains constant for different, realistic structural models are the physical processes that occur within sedimentary basins, e.g. the excitation of local surface waves and resonance effects. The frequency content and dispersion characteristics of the waves induced by these processes are clearly related to the depth of the sediments, the steepness and irregularity of the sediment-bedrock interface, and the seismic velocities.

One aspect which is not included in our discussion, is the influence of surface topography on ground motion. This approximation can be justified for sites inside sedimentary basins, where topographic features are in general small. However, topography can become important at the edges of sedimentary basins, especially in mountainous regions such as the Friuli area. Surface topography is not yet included in our numerical scheme, but can also be implemented in future, improved algorithms.

The hybrid technique, presented in this study, makes it possible (1) to study local effects even at large distances (hundreds of kilometers) from the source (Fäh, 1992), (2) to include highly realistic modelling of the source, and (3) of the propagation path. This technique, allowing parametric studies, can assist in the interpretation and prediction of ground motion at a given site. Such studies provide a complete database for the ground motion that is to be expected at sites of interest.

ACKNOWLEDGEMENTS

This study has been made possible by the CNR contracts 90.02382.CT15, 90.01026.PF54. We would like to thank ENEA for allowing us the use of the IBM3090E computer at the ENEA INFO BOL Computer Center. This research has been carried out in the framework of the activities of the ILP Task Group II.4.

REFERENCES

Alterman, Z.S. and Karal, F.C., 1968. Propagation of elastic waves in layered media by finite difference methods. Bull. Seism. Soc. Am., 58: 367-398.

Barnaba, P.F., 1978. Interpretazione geologico-strutturale della zona di Buia (Friuli). Memorie di Scienze geologiche, già Memorie degli Istituti di Geologia e Mineralogia dell'Università di Padova, Vol. XXXII: 4-13.

Ben-Menahem, A. and Harkrider, D.G., 1964. Radiation patterns of seismic surface waves from buried dipolar point sources in a flat stratified Earth. J. Geophys. Res., 69: 2605-2620.

Brambati, A., Faccioli, E., Carulli, G.B., Cucchi, F., Onofri, R., Stefanini, S. and Ulcigrai, F., 1980. Studio di microzonizzazione sismica dell'area di Tarcento (Friuli). Regione Autonoma Friuli-Venezia Giulia, Istituto di Geologia e Paleontologia dell'Università degli Studi di Trieste con la collaborazione del Politecnico di Milano.

Campillo, M., Bard, P.-Y., Nicollin, F. and Sánchez-Sesma, F.J., 1988. The Mexico Earthquake of September 19, 1985 - The incident wavefield in Mexico City during the great Michoacan earthquake and its interaction with the deep basin. Earthquake Spectra, 4: 591-608.

Clayton, R. and Engquist, B., 1977. Absorbing boundary conditions for acoustic and elastic wave equations. Bull. Seism. Soc. Am., 67: 1529-1540.

CNEN-ENEL, 1977. Accelerograms from the Friuli, Italy, earthquake of May 6, 1976 and aftershocks: Part 3, uncorrected accelerograms. Rome, Italy, November 1977.

Emmerich, H., 1992. P-SV-wave propagation in a medium with local heterogeneities: a hybrid formulation and its application. Geophys. J. Int., 109: 54-64.

Emmerich, H. and Korn, M., 1987. Incorporation of attenuation into time-domain computations of seismic wave fields. Geophysics, 52: 1252-1264.

Fäh, D., 1992. A hybrid technique for the estimation of strong ground motion in sedimentary basins. Ph.D. thesis Nr. 9767, Swiss Federal Institute of Technology, Zurich.

Fäh, D., Suhadolc, P. and Panza, G.F., 1990. Estimation of strong ground motion in laterally heterogenenous media: Modal summation - finite differences. Proc. 9-th European Conference of Earthquake Engineering, Sept. 11-16, 1990, Moscow, USSR, Vol. 4A: 100-109.

Florsch, N., Fäh, D., Suhadolc, P. and Panza, G.F., 1991. Complete synthetic seismograms for high-frequency multimode SH-waves. Pure and Applied Geophys., 136: 529-560.

Futterman, W.I., 1962. Dispersive body waves. J. Geophys. Res., 67: 5279-5291.

Giorgetti, F., 1976. An example of microseismic zoning in the Madonna di Buia area. Bollettino di Geofisica teorica ed applicata, Vol.XIX, 72: 695-706.

Giorgetti, F. and Stefanini, S., 1989. Vulnerabilità degli acquiferi del campo di Osoppo-Gemona all' inquinamento (Provincia di Udine). Istituto di Geologia e Paleontologia, Università degli Studi di Trieste, Pubblicazione n.125.

Haskell, N.A., 1953. The dispersion of surface waves on multilayered media. Bull. Seism. Soc. Am., 43: 17-34.

Knopoff, L., 1964. A matrix method for elastic wave problems. Bull. Seism. Soc. Am., 54: 431-438.

Korn, M. and Stöckl, H., 1982. Reflection and transmission of Love channel waves at coal seam discontinuities computed with a finite difference method. J. Geophys., 50: 171-176.

Levander, A.R., 1988. Fourth-order finite-difference P-SV seismograms. Geophysics, 53: 1425-1436.

Mao, W.J. and Suhadolc, P., 1987. L'area sismica del Friuli: inversione dei tempi di arrivo per un modello di velocità e modellazione di forme d'onda accelerometriche. Atti del 6° Convegno Gruppo Nazionale Geofisica della Terra Solida, CNR, Roma, Vol. I: 451-459.

Mao, W.J. and Suhadolc, P., 1992. Simultaneous inversion of velocity structures and hypocentral locations: application to the Friuli seismic area NE Italy. Pure and Applied Geophys., 138: 697-715.

Martinis, B., Carraro, F., Cavallin, A., Frascari, F., Gasperi, G., Gelmini, R., Govi, M., Manfredini, U., Panizza, M., Petrucci, F., Stefanini, S. and Zanferrari, A., 1976. The Friuli earthquake of May 6, 1976: Geology. Bollettino di Geofisica teorica ed applicata, Vol.XIX, 72: 755-808.

Panza, G.F., 1985. Synthetic seismograms: The Rayleigh waves modal summation. J. Geophysics, 58: 125-145.

Panza, G.F. and Suhadolc, P., 1987. Complete strong motion synthetics. In: B.A. Bolt (Editor), Seismic Strong Motion Synthetics. Academic Press, Orlando, Computational Techniques, 4: 153-204.

Panza, G.F., Schwab, F.A. and Knopoff, L., 1973. Multimode surface waves for selected focal mechanisms. I. Dip-slip sources on a vertical fault plane. Geophys. J. R. astr. Soc., 34: 265-278.

Poceski, A., 1969. The ground effects of the Skopje July 26, 1963 earthquake. Bull. Seism. Soc. Am., 59: 1-22.

Schwab, F., 1970. Surface-wave dispersion computations: Knopoff's method. Bull. Seism. Soc. Am., 60: 1491-1520.

Schwab, F., 1988. Mechanism of anelasticity. Geophys. J., 95: 261-284.

Schwab, F. and Knopoff, L., 1971. Surface waves on multilayered anelastic media. Bull. seism. Soc. Am., 61: 893-912.

Schwab, F. and Knopoff, L., 1972. Fast surface wave and free mode computations. In: B.A. Bolt (Editor), Methods in Computational Physics. Academic Press, New York, Vol. 11: 87-180.

Schwab, F. and Knopoff, L., 1973. Love waves and torsional free modes of a multilayered anelastic sphere. Bull. Seism. Soc. Am., 63: 1103-1117.

Slejko, D. and Renner, G., 1984. Finalità ed Esperienze della Rete Sismometrica del Friuli-Venezia Giulia. Regione Autonoma Friuli-Venezia Giulia, Trieste, pp. 75-91.

Smith, W.D., 1974. A nonreflecting plane boundary for wave propagation problems. J. Comp. Physics, 15: 492-503.

Takeuchi, H. and Saito, M., 1972. Seismic surface waves. In: B.A. Bolt (Editor), Methods in Computational Physics. Academic Press, New York, Vol. 11: 217-295.

Vaccari, F., Gregersen, S., Furlan, M. and Panza, G.F., 1989. Synthetic seismograms in laterally heterogeneous anelastic media by modal summation of P-SV waves. Geophys. J. Int., 99: 285-295.

Virieux, J., 1986. P-SV wave propagation in heterogeneous media: velocity-stress finite-difference method. Geophysics, 51: 889-901.

TABLE

Table 1. Structural model FRIUL7W, representative of the Friuli (Italy) area, obtained by damped, least-square inversion of arrival time data (Mao and Suhadolc, 1987; 1992). $Q_\alpha = 2.5\ Q_\beta$.

Thickness (km)	Density (g/cm^3)	P-wave velocity (km/s)	S-wave velocity (km/s)	Q_β
0.057	2.00	1.50	0.60	20
0.043	2.30	3.50	1.80	20
0.20	2.40	4.50	2.50	50
0.70	2.40	5.55	3.05	100
2.00	2.60	5.88	3.24	100
0.10	2.60	5.70	3.14	50
0.20	2.60	5.65	3.10	50
0.20	2.60	5.60	3.06	50
1.00	2.60	5.57	3.03	50
0.50	2.60	5.55	3.02	50
1.00	2.60	5.57	3.03	50
0.20	2.60	5.60	3.06	50
0.20	2.60	5.65	3.10	50
0.10	2.60	5.70	3.14	50
4.50	2.60	5.88	3.25	100
0.10	2.60	6.10	3.40	200
0.10	2.60	6.20	3.50	200
0.10	2.60	6.30	3.60	200
0.70	2.60	6.45	3.75	200
2.50	2.60	6.47	3.77	200
5.00	2.60	6.50	3.80	200
5.00	2.60	6.55	3.82	200
1.00	2.75	6.55	3.82	200
2.00	2.75	7.00	3.85	200
2.00	2.80	7.00	3.85	200
7.50	2.80	6.50	3.75	100
4.00	2.85	7.00	3.85	200
3.00	3.20	7.50	4.25	400
1.50	3.40	8.00	4.50	400
9.00	3.45	8.20	4.65	400

FIGURE CAPTIONS

Figure 1. Geometry of the problem with special reference to the sedimentary basin in the Friuli (Italy) area, and the September 11, 1976, Friuli aftershock ($16^h35^m04^s$).

Figure 2. Comparison of the observed ground acceleration at station Buia for the September 11, 1976 Friuli, M_L=5.7 aftershock ($16^h35^m04^s$) with the results obtained from waveform fitting with the mode summation technique for a layered, anelastic structural model:

a) Observed, uncorrected accelerograms, after Gaussian filtering, with a cutoff frequency of 6.5 Hz. The zero of the time axes does not coincide with the origin time. The amplitudes are given in cm s^{-2}.

b) Synthetic accelerograms from six point sources located at the same depth, 7.1 km, and the same distance, 15 km (Florsch et al., 1991). The strike, the angle between the strike of the fault and the epicenter-station line, the dip, and the rake are 225°, 19°, 28°, and 115°, respectively. The six point sources have different weights and time shifts (1.0, 0.6, 0.6, 0.6, 0.5, 0.5, and 0 s, 0.77 s, 1.13 s, 1.37 s, 1.9 s, 2.18 s). Weight 1 corresponds to a source with seismic moment of 1 dyne-cm. The normalized seismic moment-release in time (seismic moment rate) is shown at the bottom. The total moment $M_0=6.0 \cdot 10^{24}$ dyne-cm corresponds to the value which gives the best fit of the synthetic to the observed signals.

Figure 3. Overview of the Friuli seismic region, lining out the presence of the quaternary basin, the ISC epicenter determination of the September 11, Friuli 1976 aftershock ($16^h35^m04^s$), and the position of station Buia. The solid lines indicate the cross-sections, for which 2D modelling has been performed.

Figure 4. 2D models corresponding to cross-sections A, B and C in Figure 3, and to a model with two quarter-spaces in welded contact (cross-section D). Only the part near the surface is shown, where the models are different.

Figure 5. Acceleration time series for P-SV and SH waves at an array of receivers, for cross-section A shown in Figure 4. All amplitudes are related to a source with a seismic moment of 1 dyne-cm. The signals are normalized. The peak acceleration is indicated in units of cm s^{-2}. The distance to the source for each seismogram is given in units of km. The time scale is shifted by 2 seconds from the origin time (0 s in the figure is really 2 s from the origin time).

Figure 6. Group velocity curves of the fundamental and the first 3 higher modes of Love and Rayleigh waves for the structural model FRIUL7W.

Figure 7. Comparison between the recorded transverse, radial and vertical components of acceleration (OBS) and synthetic signals, obtained with different models (MOD: synthetic seismograms obtained for structural model FRIUL7W; ND, NC, NB, NA: synthetic seismograms obtained for model D with two layered quarter-spaces, and cross-sections C, B, and A respectively). The time-scale is shifted by 2 s from the origin time. The recorded seismograms are aligned to agree with the synthetic signals. All amplitudes of the synthetic signals correspond to a source with a seismic moment of 1 dyne-cm. The synthetic signals are normalized to the same peak acceleration which is indicated in units of cm s^{-2}.

Figure 8. Comparison between the recorded components of acceleration (OBS) and synthetic signals obtained for cross-section B. The synthetic signals have been computed for four different shear-wave velocities of the sediments (0.5 km/s, 0.6 km/s, 0.7 km/s and 0.8 km/s, as indicated at the end of each seismogram).

Figure 9. The same as in Figure 8, but for synthetic signals which have been computed for three different quality factors of the sediments (Q_β=5, Q_β=10, and Q_β=20, as indicated at the end of each seismogram).

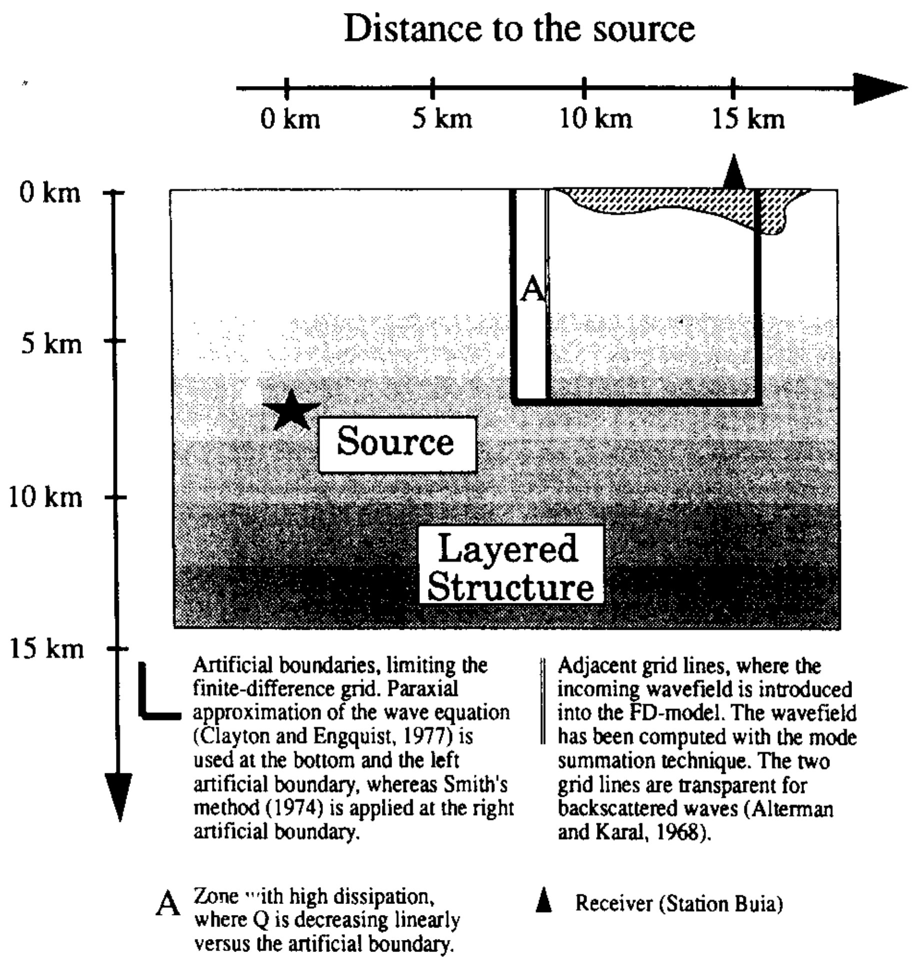
Distance to the source
0 km
5 km
10 km
15 km
0 km
5 km
10 km
15 km
A
Source
Layered Structure
Artificial boundaries, limiting the finite-difference grid. Paraxial approximation of the wave equation (Clayton and Engquist, 1977) is used at the bottom and the left artificial boundary, whereas Smith's method (1974) is applied at the right artificial boundary.
Adjacent grid lines, where the incoming wavefield is introduced into the FD-model. The wavefield has been computed with the mode summation technique. The two grid lines are transparent for backscattered waves (Alterman and Karal, 1968).
A Zone with high dissipation, where Q is decreasing linearly versus the artificial boundary.
Receiver (Station Buia)

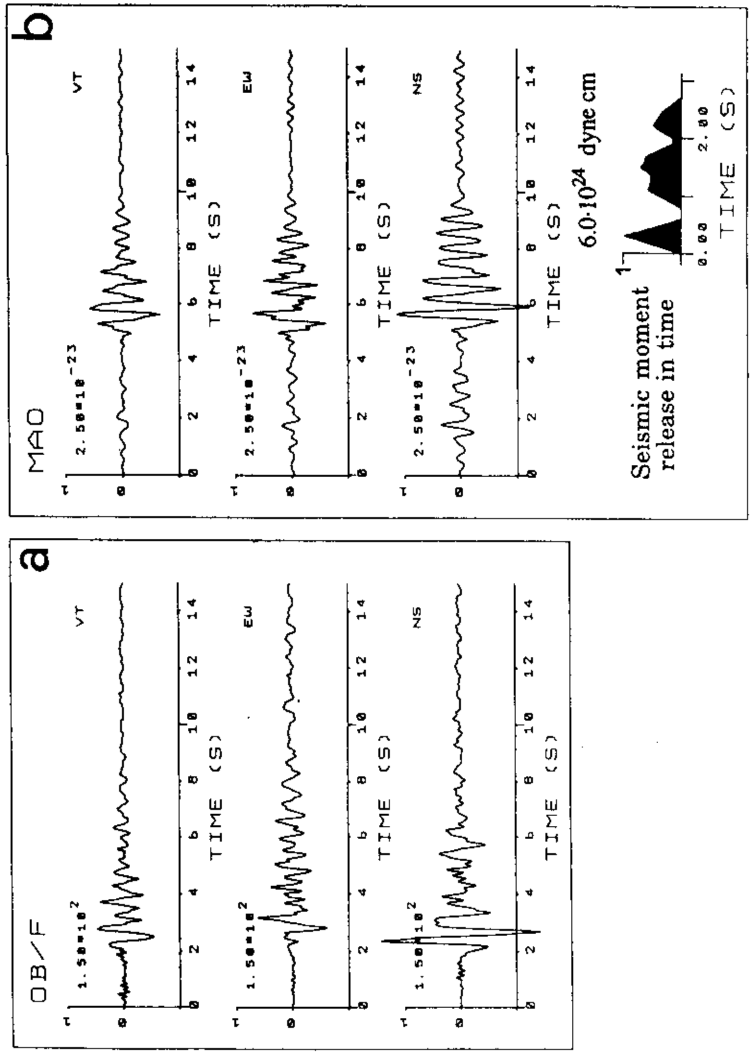
b
MAO
VT
EW
NS
TIME (S)
6.0·10^24 dyne cm
Seismic moment release in time
a
OB/F

Figure 1

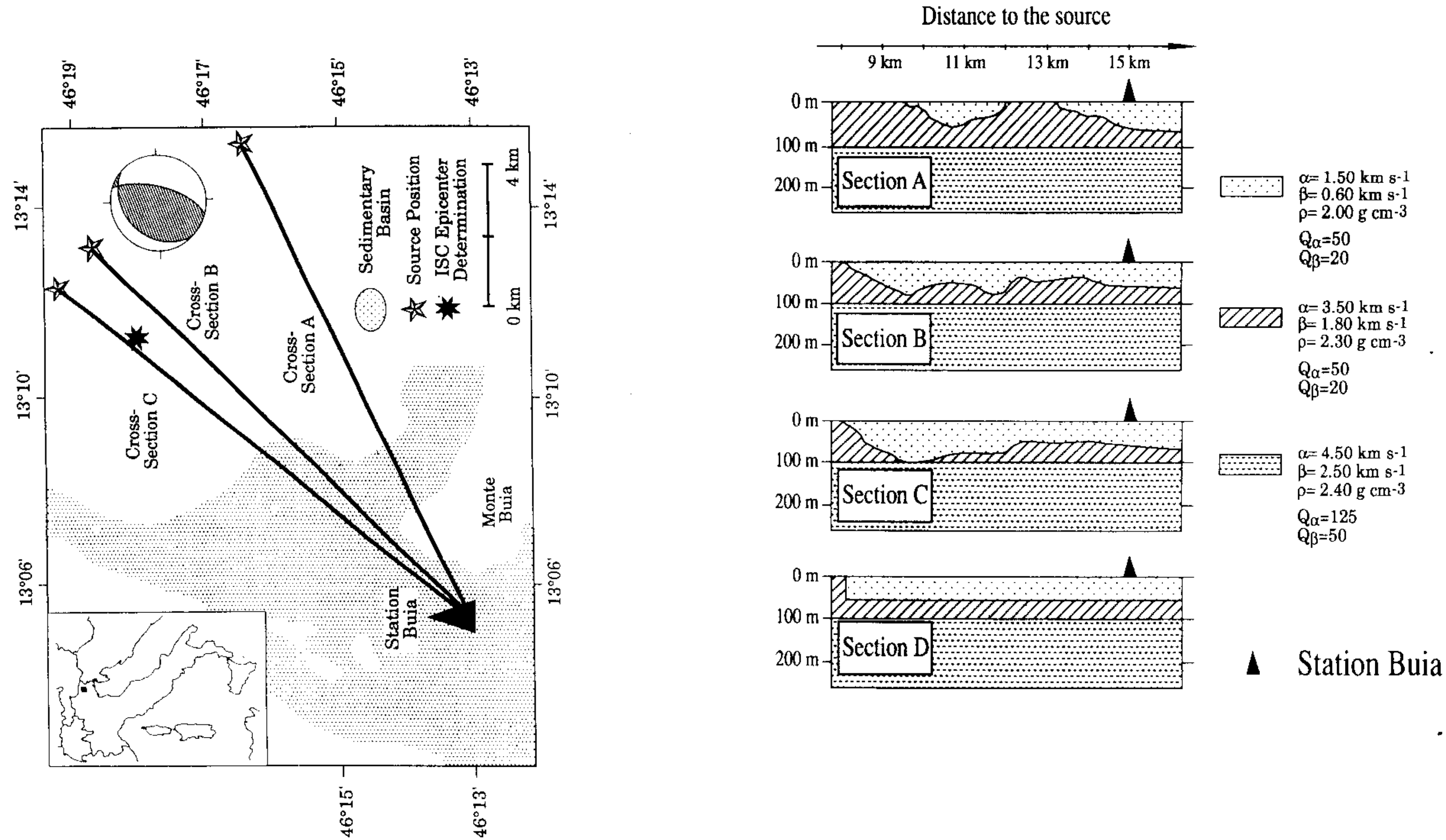

46°19'
46°17'
46°15'
46°13'
13°14'
13°10'
13°06'
Sedimentary Basin
Source Position
ISC Epicenter Determination
0 km
4 km
Cross-Section A
Cross-Section B
Cross-Section C
Monte Buia
Station Buia
Distance to the source
9 km
11 km
13 km
15 km
0 m
100 m
200 m
Section A
Section B
Section C
Section D
α= 1.50 km s-1
β= 0.60 km s-1
ρ= 2.00 g cm-3
Qα=50
Qβ=20
α= 3.50 km s-1
β= 1.80 km s-1
ρ= 2.30 g cm-3
Qα=50
Qβ=20
α= 4.50 km s-1
β= 2.50 km s-1
ρ= 2.40 g cm-3
Qα=125
Qβ=50
Station Buia

Figure 4

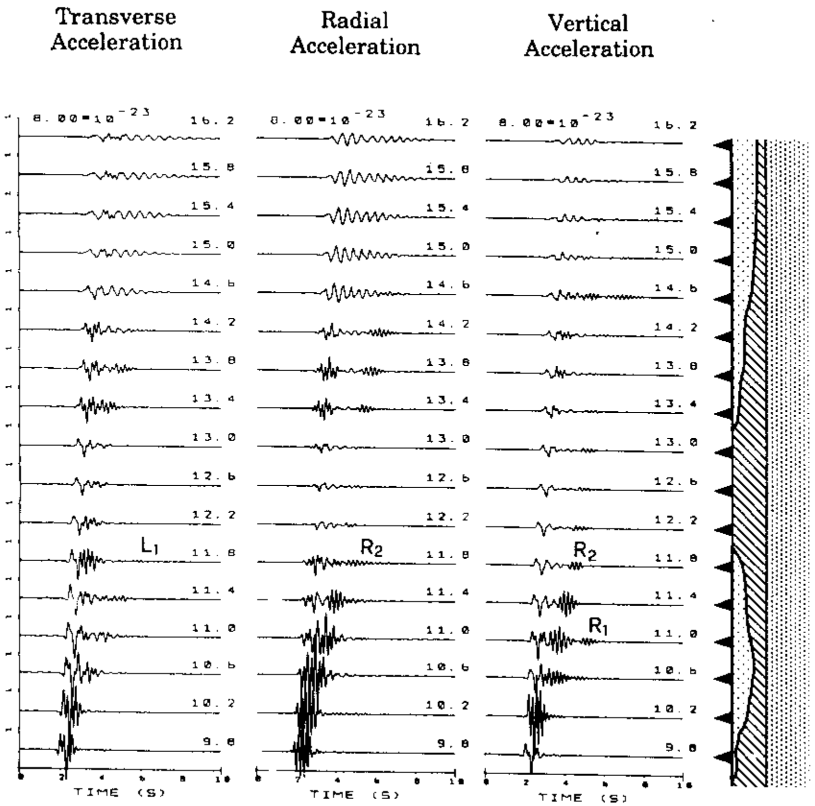

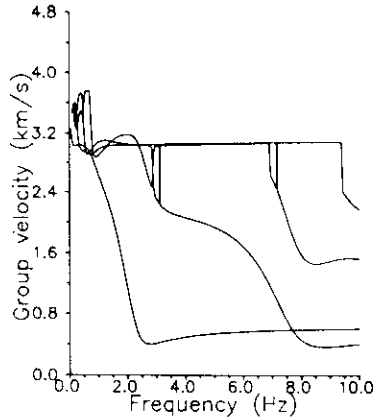

Structure: FRIUL7W
Love Modes: 0–3

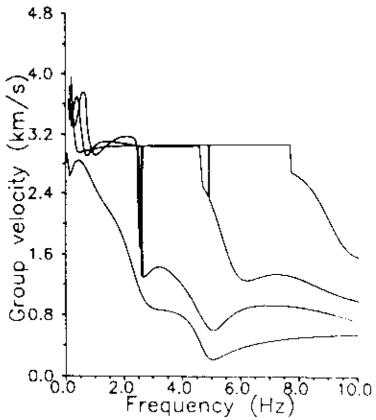

Structure: FRIUL7W
Rayleigh Modes: 0–3

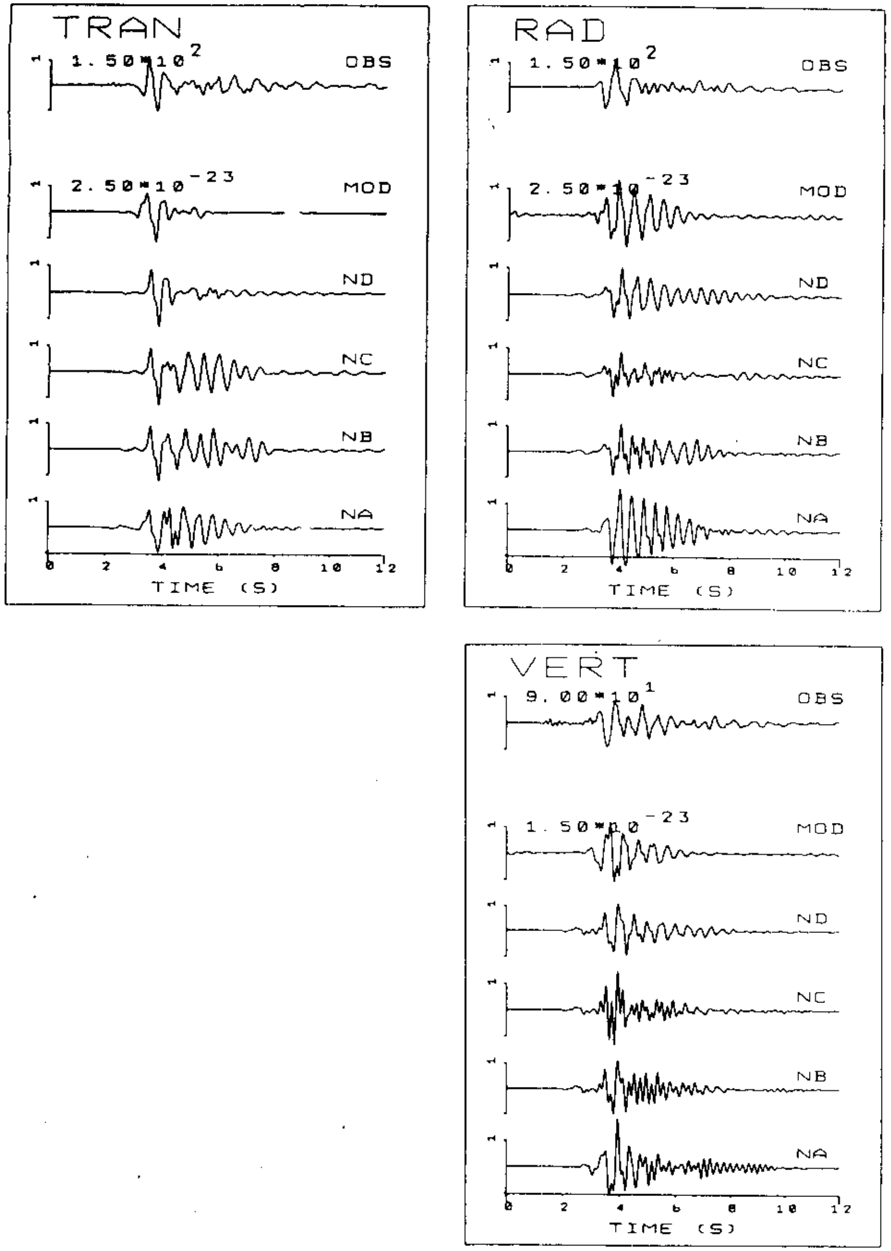
TRAN
1.50*10^2 OBS
2.50*10^-23 MOD
ND
NC
NB
NA
0 2 4 6 8 10 12
TIME (S)
RAD
1.50*10^2 OBS
2.50*10^-23 MOD
ND
NC
NB
NA
0 2 4 6 8 10 12
TIME (S)
VERT
9.00*10^1 OBS
1.50*10^-23 MOD
ND
NC
NB
NA
0 2 4 6 8 10 12
TIME (S)

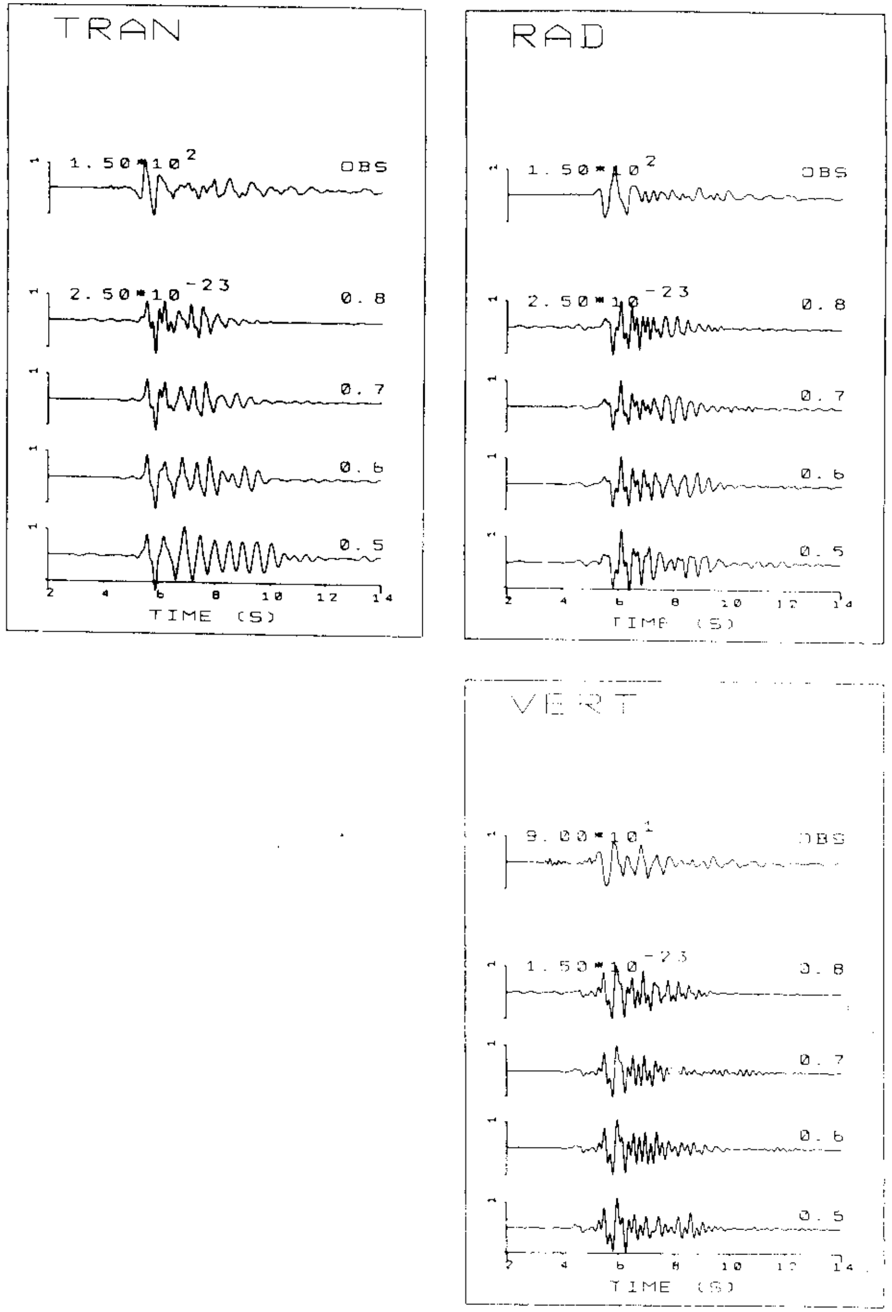
TRAN
1.50*10^2 OBS
2.50*10^-23 0.8
0.7
0.6
0.5
2 4 6 8 10 12 14
TIME (S)
RAD
1.50*10^2 OBS
2.50*10^-23 0.8
0.7
0.6
0.5
2 4 6 8 10 12 14
TIME (S)
VERT
9.00*10^1 OBS
1.50*10^-23 0.8
0.7
0.6
0.5
2 4 6 8 10 12 14
TIME (S)

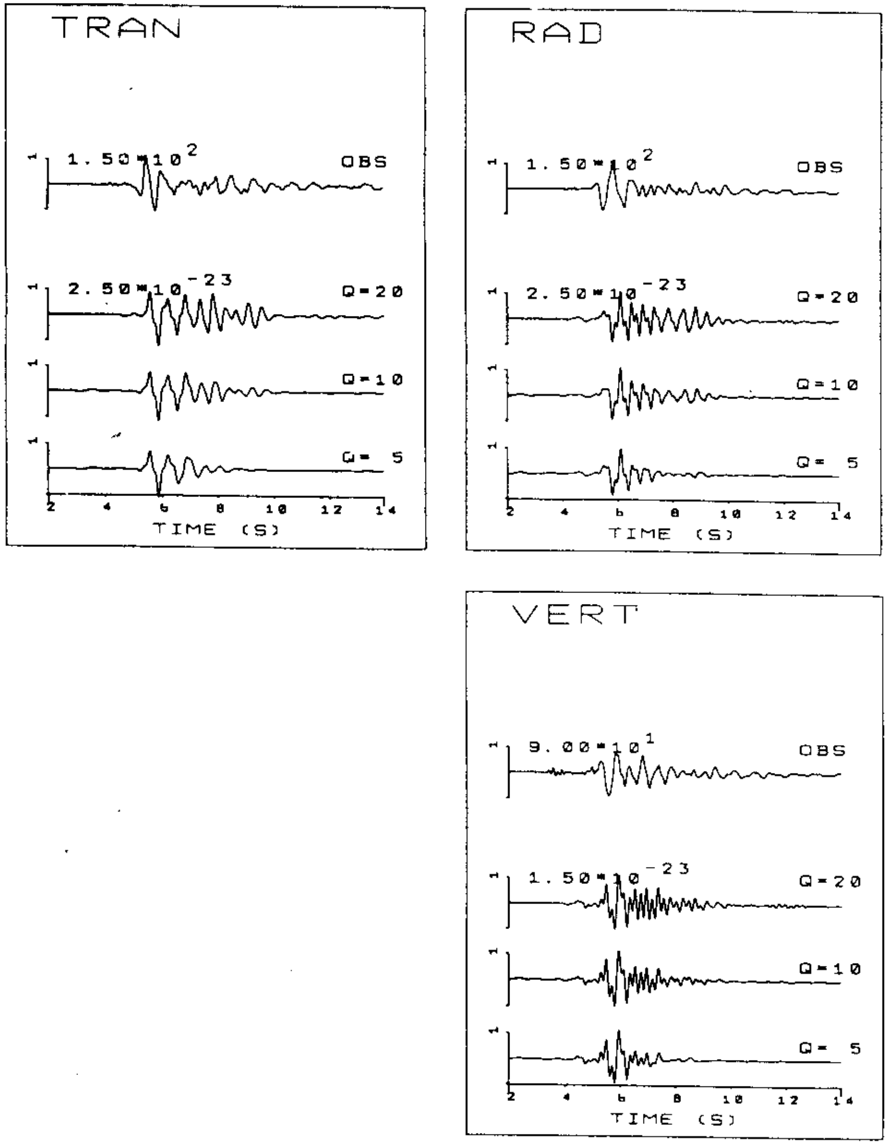
TRAN
1.50*10 2
OBS
2.50*10 -23
Q=20
Q=10
Q= 5
2 4 6 8 10 12 14
TIME (S)
RAD
1.50*10 2
OBS
2.50*10 -23
Q=20
Q=10
Q= 5
2 4 6 8 10 12 14
TIME (S)
VERT
9.00*10 1
OBS
1.50*10 -23
Q=20
Q=10
Q= 5
2 4 6 8 10 12 14
TIME (S)